

DYNAMIC SIMILARITY IN SCALING-UP FAST INTERNAL CIRCULATING FLUIDIZED BED GASIFIER

Jernej MELE, Andrej SENEGAČNIK

ABSTRACT

The article introduces research of particles dynamics in a cold flow model of FICFB (Fast Internal Circulating Fluidized Bed) biomass gasification process and its scale-up to hot industrial pilot plant. A laboratory unit has been made for the purposes of experimental research, which is three times smaller than the industrial pilot plant. Process was designed and experimentally tested on cold-flow model and scaled-up to hot industrial process. For a reliable scaling up similar flow conditions were achieved in both units. The results of the laboratory model shows as similar to those of the scale-up device if geometry, flow and Reynolds numbers are the same. Therefore, there is no need to bring an expensive full-scale gasification plant into the laboratory and actually test it. This is an example of "dynamic similarity".

POVZETEK

Članek predstavlja praktično uporabo teorije podobnosti pri načrtovanju uplinjevalnika biomase v lebdečem sloju. Obravnavana je hidrodinamika trdnih delcev v hladnem modelu FCIFB (hitro krožeče lebdeče plasti) uplinjevalnika, ki je s teorijo podobnosti ekstrapolirana na vročo industrijsko pilotno napravo. Za laboratorijske raziskave krožeče lebdeče plasti je bila izdelana laboratorijska naprava, ki je trikrat manjša od industrijske in deluje pri temperaturi okolice. Stabilnost hitro krožeče lebdeče plasti med dvema reaktorjema je bila eksperimentalno preverjena v laboratorijski napravi in nato ekstrapolirana na vroč industrijski proces. Pri dimenzioniranju naprav sta bila v obeh napravah vzpostavljena podobna tokova, s podobno geometrijo in podobnimi Reynoldsovimi števili. Eksperimentalni rezultati laboratorijske in pilotne naprave so medsebojno ustrezno primerljivi. Izvedeni primer dinamične podobnosti potrjuje, da ni potrebno vmesno izdelovanje drage industrijske pilotne naprave za laboratorijsko testiranje.

1. INTRODUCTION

While researching the 750kW FICFB gasification pilot plant certain questions concerning particle dynamics in gas flows arose. The flow dynamic of FICFB cannot be exactly

analytically or numerically modelled. Building a pilot plant draws high expenses and therefore we must be quite certain that the pilot apparatus will perform planned task.

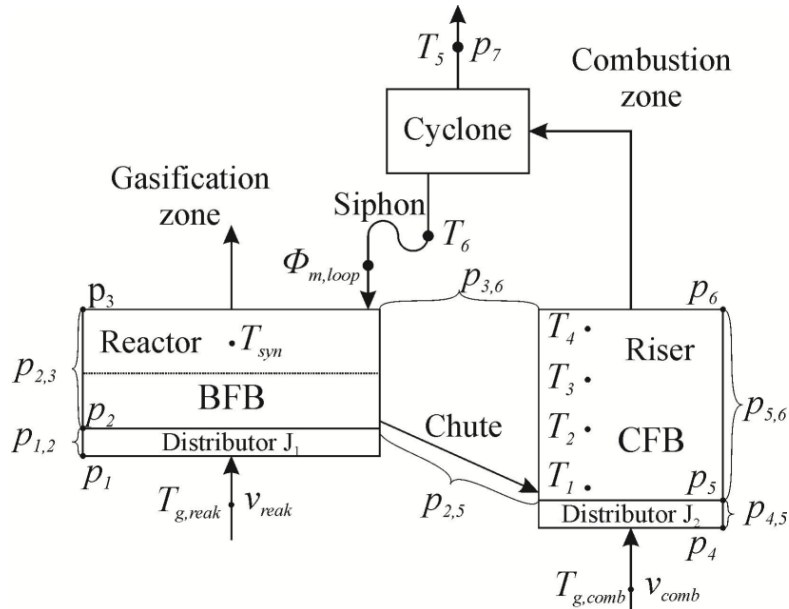


Fig. 1: Scheme of FICFB laboratory and pilot system

The gasification process is distributed into two (fluidized bed) reactors/zones (Fig. 1), a gasification zone and a combustion zone. The solid fuel is fed into the gasification zone fluidized with superheated steam. The bed material together with some remaining charcoal moves to the combustion zone through the chute. In combustion zone the remaining carbon burns and heat up the bed material (catalyst). Hot bed material is pneumatically transported through the riser to the cyclone where is separated and collected in a siphon. Siphon fully filled with hot bed material acts as a gas barrier between reactors i.e. syngas and flue gas. With this concept it is possible to get a high-grade product synthetic gas without use of pure oxygen. The system is patented with European patent EP 2 146 143 A2 [1].

2. EXPERIMENTAL EQUIPMENT

2.1 Cold-flow model

Cold-flow model is a laboratory unit dimensional three times smaller than the pilot plant. Its main purpose was to simulate the hydrodynamic process of FICFB gasification with air at arbitrary conditions. It is made from stainless steel and glass, so that the particle behaviour can be observed. Fig. 2 shows a model of laboratory unit.



Fig. 2: Laboratory unit



Fig. 3: Pilot plant in operation, on the left flame of syngas torch burning

2.2 FICFB Pilot plant

The pilot plant (Fig. 3) is designed according to heavy thermal and abrasive conditions which occur in it. Gas chambers are made of heat resistant stainless steel and protected with thermo concretes so that hot gas-solid flow does not trite the steel walls. Main gas inlets are superheated water steam and air, main outlets are hot flue gas from cyclone and syngas from the reactor. All gas flows are measured with orifices. FICFB pilot plant is 3 times larger and cost 50 times more than the cold-flow model.

3. THEORY

Two physical phenomena or processes are similar if at corresponding moments of time at corresponding points, the values of the variable quantities that characterize the system state are proportional to the corresponding quantities of the second system. In similarity theory we know few types of similarities like geometrical, kinematical, dynamical, thermal, chemical, economical, etc. Praxis shows us that all criteria of similarity cannot be satisfied. In other words all similarity factors between laboratory and industrial process cannot be alike. Process designers have to determine which factors should be considered.

In this case dynamic similarity will be studied because the most important is that the system runs properly. First the inner circulation flows and fluidization should be treated after that the energy and mass balance too.

3.1 Dynamic similarity

The goal herein is to compare flows in the laboratory unit and in the pilot plant. In order for the two flows to be similar they must have the same geometry and equal particle Reynolds numbers [2]. When comparing fluid behaviour at homologous points in a model and a full-scale flow, the following holds:

$$Re_p(\text{laboratory unit}) = Re_p(\text{Scale-up pilot plant})$$

In general, a particle Reynolds number Re_p has the form:

$$Re_p = \frac{d_p \cdot v_g \cdot \rho_g}{\eta_g} \quad (1)$$

Where: d_p – average particle diameter, v_g – gas velocity, ρ_g – gas density, η_g dynamic viscosity of gas

Many authors suggested analytical correlations for determining the Re_p . For review of these correlations see Gupta et.al. (2009) [3]. Wen and Yu suggested using the following equation to calculate the Reynolds number of minimum fluidization:

$$Re_{pmf} = \sqrt{33,7^2 + 0,0408 \cdot Ar} - 33,7 \quad (2)$$

Where the Archimedes number Ar is defined as [4]:

$$Ar = \frac{d_p^3 \cdot \rho_g (\rho_s - \rho_g) \cdot g}{\eta^2} \quad (3)$$

3.2 Fluidizing velocities

Full fluidization is a regime when all the particles start to fluidize. It occurs in conical and non-conical beds and/or with wide size distribution of particles. When we have wide size distribution of particles, the smaller and lighter particles start to fluidize and slip into the empty spaces between the larger particles, while the larger particles remain stationary. For small particles and low Reynolds numbers the viscous energy losses predominate. For the estimation of minimal fluidization velocity v_{mf} we use Ergun's equation where ϕ_s is particle sphericity, d_p average diameter of particles, ρ_p density of particles, ρ_g gas density, η_g dynamic gas viscosity and ε_{mf} bed voidage. [4]:

$$v_{mf} = \frac{(\Phi_S \cdot d_p)^2 \cdot (\rho_p - \rho_g) \cdot g \cdot \varepsilon_{mf}^2}{150 \cdot \eta_g} \quad \text{for } Re_p < 20 \quad (4)$$

For large particles only the kinetic energy losses need to be considered:

$$v_{mf} = \sqrt{\frac{\Phi_S \cdot d_p \cdot (\rho_p - \rho_g) \cdot g \cdot \varepsilon_{mf}^3}{1,75 \cdot \eta_g}} \quad \text{for } Re_p > 1000 \quad (5)$$

If Φ_S and ε_{mf} are unknown, the following modifications suggested by *Wen and Yu* [4] can be used:

$$\frac{1 - \varepsilon_{mf}}{\Phi_S^2 \cdot \varepsilon_{mf}^2} \cong 11 \quad (6)$$

and

$$\frac{1}{\Phi_S \cdot \varepsilon_{mf}^3} \cong 14 \quad (7)$$

Equations (4) and (5) can now be simplified to:

$$v_{mf} = \frac{d_p^2 \cdot (\rho_p - \rho_g) \cdot g}{1650 \cdot \eta_g} \quad \text{for } Re_p < 20 \quad (8)$$

$$v_{mf} = \sqrt{\frac{d_p \cdot g \cdot (\rho_p - \rho_g)}{24,5 \cdot \rho_g}} \quad \text{for } Re_p > 1000 \quad (9)$$

The upper limit of gas flow rate is approximated by the terminal (free fall) velocity of the particles v_t , which can be estimated from the fluid mechanics [4]:

$$v_t = \sqrt{\frac{4 \cdot g \cdot d_p^3 \cdot (\rho_p - \rho_g)}{3 \cdot \rho_g \cdot C_x}} \quad (10)$$

There are spherical and non-spherical particle shapes in the bed and each of them has a different drag coefficient value C_x . If we combine equations (1) and (10) we get the velocity independent group:

$$C_x \cdot Re_p^2 = \frac{4 \cdot g \cdot d_p^3 \cdot \rho_g \cdot (\rho_p - \rho_g)}{3 \cdot \eta_g^2} \quad (11)$$

An alternative way of finding v_t for spherical particles uses analytical expressions for the drag coefficient C_x [4].

$$v_t = \frac{(\rho_p - \rho_g) \cdot g \cdot d_p^2}{18 \cdot \eta_g} \quad \text{for } Re_p < 0,4 \quad (12)$$

$$v_t = \sqrt[3]{\frac{4}{225} \frac{(\rho_p - \rho_g)^2 \cdot g^2}{\rho_g \cdot \eta_g}} \cdot d_p \quad \text{for } 0,4 < Re_p < 500 \quad (13)$$

$$v_t = \sqrt{\frac{3,1 \cdot d_p \cdot (\rho_p - \rho_g) \cdot g}{\rho_g}} \quad \text{for } 500 < Re_p < 200000 \quad (14)$$

But still no simple expression can represent the experimental findings for the entire range of Reynolds numbers, so by replacing these values C_x in equation (11) we obtain:

$$v_t = \frac{(\rho_p - \rho_g) \cdot g \cdot d_p^2}{18 \cdot \eta_g} \quad \text{for } Re_p < 0,4 \quad (15)$$

$$v_t = \sqrt[3]{\frac{4}{225} \frac{(\rho_p - \rho_g)^2 \cdot g^2}{\rho_g \cdot \eta_g}} \cdot d_p \quad \text{for } 0,4 < Re_p < 500 \quad (16)$$

$$v_t = \sqrt{\frac{3,1 \cdot d_p \cdot (\rho_p - \rho_g) \cdot g}{\rho_g}} \quad \text{for } 500 < Re_p < 200000 \quad (17)$$

3.3 Pressure drops

Estimation of pressure drop across the fluidized beds is very important for dimensioning actuators (for example: blower or steam generator) and measuring components. This estimation gains further importance when designing the industrial processes. For the estimation of pressure drop across the conical beds we use modified Ergun's equation where geometric characteristic effects are included [5]. All the symbols are presented in Fig. 5.

$$\Delta p = A \cdot (L - h_b) \cdot \frac{r_0^2}{r_1 r_b} v_{g0} + B \cdot (L - h_b) \frac{r_0^4 \cdot (r_b^2 + r_b r_1 + r_1^2)}{3 r_1^3 r_b^3} \cdot v_{g0}^2 + (1 - \varepsilon)(\rho_s - \rho_g) \cdot g \cdot h_b + \frac{1}{2} v_{g0}^2 \cdot \left[\left(\frac{1}{\varepsilon_f} \right)^2 \left(\frac{r_0}{r_1} \right)^4 - \left(\frac{1}{\varepsilon_{pf}} \right)^2 \right] \cdot \rho_g \quad (18)$$

$$A = 150 \frac{(1 - \varepsilon_{mf})^2}{\varepsilon_{mf}^3} \cdot \frac{\eta_g^2}{(\Phi_s d_p)^2} \quad (19)$$

$$B = 1.75 \frac{1 - \varepsilon_{mf}}{\varepsilon_{mf}^3} \cdot \frac{\rho_g}{\Phi_s d_p} \quad (20)$$

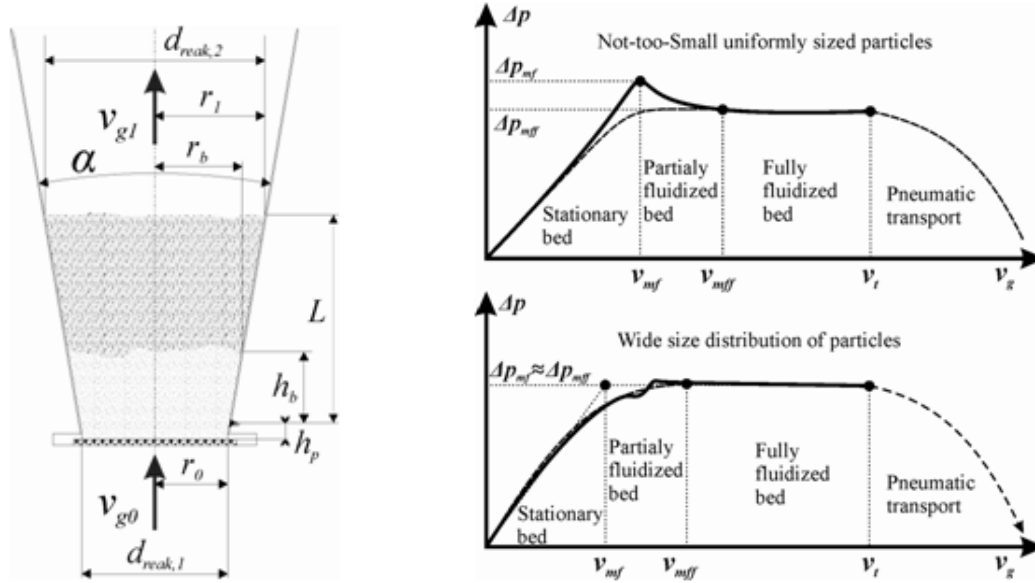


Fig. 4: Characteristic reactor dimensions with pressure characteristics

With an increased gas velocity a characteristic pressure curve occurs. Pressure drop starts to increase reaching its maximum value Δp_{mf} at minimum fluidization velocity v_{mf} . When the bed is fully fluidized (at v_{mff}), the pressure drop is reduced to Δp_{mff} and is almost constant until the gas reaches terminal velocity. This usually applies to Not-too-Small Uniformly Sized Particles (Fig. 4). For industrial cases we can use the simplified equation [5]:

$$\Delta p_{mff} = (1 - \varepsilon_{mff})(\rho_s - \rho_g) \cdot g \cdot L_{mff} \quad (21)$$

A somewhat different pressure drop characteristic occurs with a wide size distribution of particles, which are usually present in industrial processes. When the gas velocity increases through the bed of solids, the smaller particles start to fluidize and slip into the void spaces between the larger particles, while the larger particles remain stationary [6] (see Fig. 4).

4. SCALING UP

On the basis of the previously-mentioned equations, we can make an estimation of flow conditions in the reactor and combustion zone. We have made a comparison of physical properties between the laboratory unit and pilot plant in Tables 2 and 3. The comparison is based on the established equality of Reynolds numbers. Glicksman [2, 7] pointed out that for designing an accurate scale model of a given fluidized bed all of the independent non-dimensional parameters should be even. Operating temperature of the pilot plant is much higher and therefore the influence on transport properties should be considered. In the

laboratory unit flows are generated with upward-blowing air at arbitrary conditions whereas in the pilot plant the bed material is fluidized with superheated steam and in the riser with hot air.

In the meantime endothermic chemical reactions of pyrolysis and a water-gas-shift reaction will take place in the reactor while exothermic combustion occurs in the combustion zone. Flue gases exits combustion zone with temperature $\approx 900^\circ\text{C}$ and syngas the reactor with $\approx 800^\circ\text{C}$. Gases in the pilot plant have lower densities and higher viscosities than the air in the laboratory unit. The bed material is quartz sand with average diameter of 400-600 μm . In order to establish similar conditions, we have to use smaller particles in the lab unit - quartz sand with average particle diameter of 100-300 μm . On the basis of studied flows on the lab unit – velocities, mass flows and pressure drops through distributors and fluid beds, we may anticipate similar flow characteristics in the pilot plant.

In industrial applications the flow of fluidizing fluid is typically chosen as a function of the desired fluidization state and the required mass and energy balances, etc. [4] and not as a function of the minimum gas velocity to fluidize all the particles. However, if we look at equations 8 and 9 we can see that only variable is gas velocity v_g or v_{mf} . At designing or scaling up the pilot plant we can adjust the desired fluidization state at required mass flow with inside reactor diameters and geometry.

5. EXPERIMENTAL WORK

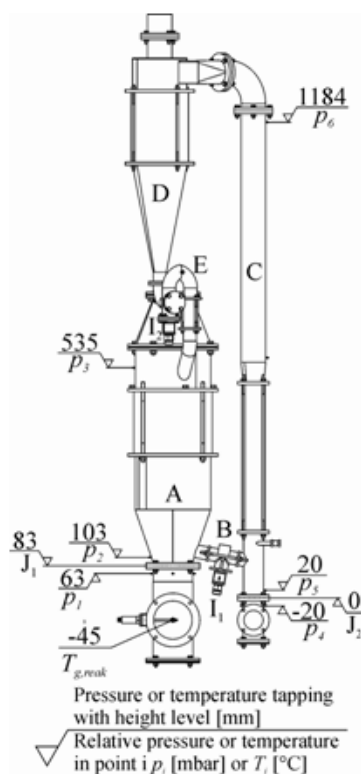


Fig. 5: Pressure measuring points in cold-flow model

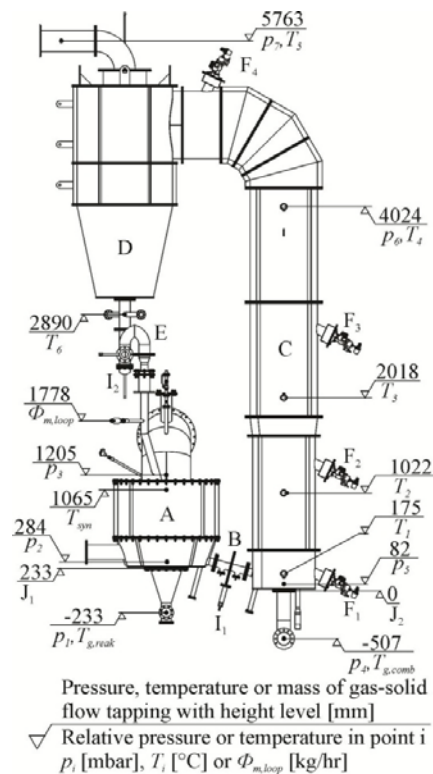


Fig. 6: Pressure measuring points in pilot plant

The continuous gasification process was achieved during stable particle circulation. In the reactor (A) a bubbling fluidized bed was established. Angle of the chute (B) is designed so, that there is no solid flow if the particles are not fluidized. All the particles transported to combustion cone (C) are pneumatically lifted to the cyclone (D) and heated up. With long dwelling times of particles in the combustion cone, we want that the particles collect as much heat as possible. Red-hot particles are separated from the flue gases in cyclone and finally gathered in siphon (E). The auxiliary inlet (I_2) acts to fluidize the gathered hot particles and transport them to the reactor (Fig. 5, Fig. 6). Process is controlled with traditional method – pressure drop across the bed versus superficial gas velocity. For the process driving pressures and temperatures monitoring are vital. We have installed the Endress+Hauser PDM75 and Siemens Sitrans 250 delta bars for on-line pressure measurements and ECOM UNO 1545 for manual pressure measurements. Temperatures are measured with 2K (NiCr-Ni) thermocouples. Pilot plant has installed the solid-flow sensor SWR SolidFlow FSM for detection of mass particle flow. All the gas flows are measured with orifices. Measuring scheme and location points are presented in Fig. 1, 5 and 6.

Table 2: Technical and process data of cold-flow model and pilot plant reactor

Parameter	Symbol	Cold-flow model	Pilot plant	
Reactor diameter at gas entrance	$d_{reak,1}$ [mm]	100	300	
Reactor diameter above the fluidized bed	$d_{reak,2}$ [μm]	190	600	
Conical bed angle	α [°]	40	40	
Gas distributor type		Sandwiching nets	Bubble cap	
Bed material		Quartz sand	Quartz sand	
Particle size	d_p [μm]	100—300	400—600	
Geldard's classification		lower B	middle B	
Particle density	ρ_p [kg/m ³]	2650	2650	
Bulk density	$\rho_{p,b}$ [kg/m ³]	1575	1550	
Stationary bed height	L [mm]	130	400	
Fluidization medium		Air	Steam*	Syngas**
Temperature	$T_{g,reak}$ [°C]	40°C	550	780
Density [8]	ρ_g [kg/m ³]	1.124	0,288	0,192
Dynamic viscosity [8]	η_g [Pas]	$1.8 \cdot 10^{-5}$	$3.1 \cdot 10^{-5}$	$4.6 \cdot 10^{-5}$
Volume flow of fluidization medium	$\Phi_{v,reak}$ [m ³ /h]	31.1	517.1	4275
Gas velocity (experimental)	v_{reak} [m/s]	1.11	2.03	6.05
Gas velocity (predicted)	v_{mff} [m/s]	0.397	1.40	1.66
Pressure drop (experimental)	Δp_{reak} [mbar]	13.5	47.8	47.8
Pressure drop (predicted)	Δp_{reak} [mbar]	13.9	42.6	42.6
Reynolds number (Calculated)	Re_p	14.0	25.1	12.6

* Gas inlet at the bottom of the reactor

** Gas outlet above the fluidized bed in the reactor

6. EXPERIMENTAL RESULTS

Centre of this scientific work is research of fluidized bed particle dynamics in laboratory unit and its scale-up to industrial pilot plant. We have monitored the vital relative pressures, temperatures and gas flows in both units at the stable loop. Results are presented in Table 3. They show how pressures are distributed across the system in cold-flow model and pilot plant. Pilot plant is designed to have similar gas-particle flow characteristics as cold-flow model. Pressure p_2 at the bottom of the fluidized bed is larger than that at the point where the chute connects to the combustion zone p_5 . The gas-solid flow direction is from the reactor to the combustion zone, pushing the particles in the desired direction. At the top of the fluidized bed we have pressure p_3 which is desired (not demanded) to be lower than p_6 or p_7 , so the particles can travel back to the reactor. There has to be enough material in the siphon at all time in order to prevent mixing of gases between the zones. Therefore, the siphon has to serve as seal gap for gases but not for material [9, 10].

Table 3: Experimental results on cold-flow model and pilot plant at stable loop or at working stadium

Parameter	unit	Cold-flow mod.	Pilot plant
p_1	mbar	36.6	410.0
p_2	mbar	13.7	48.6
p_3	mbar	0.2	0.2
p_4	mbar	6.2	315.0
p_5	mbar	3.9	10.6
p_6	mbar	3.2	6.6
p_7	mbar	0.1	4.9
$T_{g,reak}$	°C	42	628
$T_{g,comb}$	°C	42	53
T_1	°C	N/A	480
T_2	°C	N/A	677
T_3	°C	N/A	736
T_4	°C	N/A	728
T_5	°C	N/A	786
T_6	°C	N/A	797
T_{syn}	°C	N/A	727
$\Phi_{m,loop}$	kg/hr	N/A	562
$\Phi_{V,gas}$	m ³ /h	31.1	4275
$\Phi_{V,comb}$	m ³ /h	70	5913

In cold flow model experiments were made when testing the process with quartz sand where the average particle diameter was about 200 μm . The stationary bed height in the reactor was 130 mm and the mass of sand used at simulation was 4.25 kg. The pressure drop across the fluidized bed was $p_{2,3} = 13.5$ mbar. Air flow had an average temperature of 42°C. Superficial gas velocity is about 1.11 m/s in the reactor and 9.8 m/s in the combustion zone. Pilot plant had a higher bed which was about 400 mm of quartz sand with average diameter of 500 μm . We can see that the pressure drop across the bed is approximately $p_{2,3} = 48.4$ mbar. Superficial gas velocity is about 2.03 m/s at the bottom of the bed and 6.05 m/s above the bed. Increase of superficial velocity is consequential to production of syngas in the reactor, which results in the increase of gas volume. It shows us that the tapered bed could have larger angle α . Similar results can be seen in the combustion cone, where increase of superficial velocity is even larger – from 12.6 to 57.9 m/s.

7. CONCLUSIONS

Modern gasification systems are using fluidized beds. Its advantage is more homogenous temperature profile in the bed, better heat transfer and possible use of catalyst. It lends itself to complete combustion applications which would allow it to use liquid wastes, such as used engine oil, non-recyclable plastics, junk mail & old shoes and garbage for the generation of heat. However, there is a problem of complex design and regulation. By observing the FICFB processes in a three-time smaller laboratory unit with air as a driving fluid the size and density of bed particles has been determined. The assumption of particle flow similarity is based on a direct comparison of particle Reynolds numbers. Dynamic similarity was achieved by using different particle size in process. Chemical reactions cause variations in temperature, density, and dynamic viscosity all of which affect Re_p . If we compare Re_p at the reactor inlet 14.0 and 25.1 at the outlet, we can see that Re_p changes by 55 % and the similarity at this point is actually questioned. When the process is stabilized and a smooth circulation is established, the pressure relations are as expected and all of the gas flows are pouring in the appropriate directions. The scale up procedure is affirmed with successful demonstration of FICFB pilot plant located in Celje, Slovenia.

8. ACKNOWLEDGEMENTS

Operation was partially financed by the European Union, European Social Fund and European Regional Development Fund.

9. REFERENCES

- [1] Bosch, Klaus, Verfahren und Vorrichtung zur Erzeugung eines stickstoffarmen bzw. nahezu stickstofffreien Gases, EP 2 146 143 A2, filed Jul 16, 2009 and issued Jan 20, 2010.

- [2] Leon R. Glicksman (1982), *Scaling Relationships For Fluidized Beds*, Chemical engineering science, 39, 1373-1384
- [3] Gupta S. K., Agarwal V. K., Singh S. N., Seshadri V., Mills D., Singh J., Prakash C., *Prediction of minimum fluidization velocity for fine tailing materials*, Powder Technology 196 (2009) 263-271
- [4] Daizo Kunii, Octave Levenspiel, *Fluidization Engineering*, John Wiley & Sons, inc., 1969
- [5] Rachadaporn Kaewklum, Vladimir I. Kuprianov, *Theoretical And Experimental Study On Hydrodynamic Characteristic Of Fluidization In Air-Sand Conical Beds*, Chemical Engineering Science 63 (2008) 1471-1479
- [6] Janez Oman, *Generatorji Toplote*, University in Ljubljana, Faculty of mechanical engineering, Ljubljana, 2005
- [7] M. T. Nicastro, Leon R. Glicksman (1982), *Experimental Verification of Scaling Relationships for Fluidized Beds*, Chemical engineering science, 39, 1373-1384
- [8] Janez Oman, A. Senegačnik, A. Mirandola, *Air, Fuels and Flue Gases: Physical Properties and Combustion Constants*, Edizioni Libreria Progeto, Padova, Italy, 2006
- [9] G. Löffler, S. Kaiser, K. Bosch, H. Hofbauer (2003), *Hydrodynamics of a Dual Fluidized - Bed Gasifier - Part I : Simulation of a Riser With Gas Injection and Diffuser*, Chemical Engineering Science, 58, 4197 – 4213
- [10] S. Kaiser, G. Löffler, K. Bosch, H. Hofbauer (2003), *Hydrodynamics of a Dual Fluidized Bed Gasifier - Part II: Simulation of Solid Circulation Rate, Pressure Loop and Stability*, Chemical Engineering Science, 58, 4215 – 4223

AUTHORS ADDRESSES

Jernej Mele, b.sc. mech.eng.

Assoc. prof. dr. Andrej Senegačnik *

Bosio d.o.o., Obrtniška cesta 3, 3220 Štore, SLOVENIA

*University of Ljubljana, Faculty of Mechanical Engineering, Aškerčeva 6, 1000 Ljubljana, SLOVENIA

Tel: +00386 1 4771 313

e-mail: jernej.mele@bosio.si, andrej.senegacnik@fs.uni-lj.si